

RESONANCE INTEGRALS OF ENGINEERING MATERIALS

by

Thomas A. Greene

A Thesis Submitted to the Faculty of the

DEPARTMENT OF NUCLEAR ENGINEERING

In Partial Fulfillment of the Requirements
For the Degree of

MASTER OF SCIENCE

In the Graduate College

THE UNIVERSITY OF ARIZONA

1 9 6 9

STATEMENT BY AUTHOR

This thesis has been submitted in partial fulfillment of requirements for an advanced degree at The University of Arizona and is deposited in the University Library to be made available to borrowers under rules of the Library.

Brief quotations from this thesis are allowable without special permission, provided that accurate acknowledgment of source is made. Requests for permission for extended quotation from or reproduction of this manuscript in whole or in part may be granted by the head of the major department or the Dean of the Graduate College when in his judgment the proposed use of the material is in the interests of scholarship. In all other instances, however, permission must be obtained from the author.

SIGNED: Thomas A Greene

APPROVAL BY THESIS DIRECTOR

This thesis has been approved on the date shown below:

M. V. Davis

M. V. DAVIS

Professor of Nuclear Engineering

February 1, 1969

Date

ACKNOWLEDGMENTS

The author would like to express his sincere appreciation to Dr. M. V. Davis for his valuable suggestions and advice during the course of this work.

The author is also indebted to Mr. Paul S. Pickard for his advice and for his numerous hours spent in operating the reactor.

TABLE OF CONTENTS

	Page
LIST OF TABLES	v
LIST OF ILLUSTRATIONS	vi
ABSTRACT	vii
1. INTRODUCTION	1
2. THEORETICAL DEVELOPMENT	4
3. EXPERIMENTAL PROCEDURE	9
4. REACTIVITY MEASUREMENT	11
5. PREPARATION OF SAMPLES	14
6. RESULTS	17
7. SUMMARY AND CONCLUSION	22
APPENDIX I: SELF-SHIELDING	24
APPENDIX II: COMPUTER PROGRAM	26
APPENDIX III: ADJOINING FLUX	31
APPENDIX IV: PARAMETERS OF MATERIALS USED IN CALCULATIONS	33
REFERENCES	36

LIST OF TABLES

	Page
TABLE I: SAMPLE DIMENSIONS AND WEIGHTS	16
TABLE II: REACTIVITY MEASUREMENTS OF GOLD SAMPLES	17
TABLE III: REACTIVITY CORRECTIONS	18
TABLE IV: REACTIVITY MEASUREMENTS OF SAMPLE MATERIALS	21
TABLE V: PARAMETERS OF RESOLVED GOLD RESONANCE	35

LIST OF ILLUSTRATIONS

	Page
FIGURE 1: Measured Reactivity Versus Mass of Gold	19
FIGURE 2: Adjoint Flux Versus Neutron Energy	32

ABSTRACT

A method of determining the cadmium cutoff energy is developed by the ratio of the reactivity of a $1/v$ absorber to that of a resonance absorber. An equation is derived to calculate the cutoff energy by assuming the adjoint function is independent of energy. After the cutoff energy has been determined, by using the known resonance of gold as a standard, the resonance integral of tantalum, tungsten, stainless steel 304 and 416 are calculated by two methods. The results of both methods are compared and discussed.

CHAPTER 1

INTRODUCTION

A resonance integral is defined as "the integral of the absorption cross section over the resonance region which is necessary to account for the observed neutron absorption rate in a flux equal to that existing in the absence of the resonance."(1) This may be stated mathematically as

$$I = \int [\sigma_a(E)]_{\text{eff}} \phi dE \rightarrow \int [\sigma_a(E)]_{\text{eff}} \frac{dE}{E}$$

where

I = resonance integral

$[\sigma_a(E)]_{\text{eff}}$ = effective absorption cross section

E = energy

ϕ = neutron flux

The measurement of resonance integrals has played an important role in the development of reactor physics since the first "pile danger method" to the present day methods which determine the effect of fuel, moderator and structural materials on criticality in both thermal and fast reactors. Several methods have been used in the past for the determination of resonance integrals of various substances. Three of the most common methods are:

1. Measurement of the reactivity changes caused by oscillating a sample inside a cadmium tube in a reactor.

2. Measurement of the reactivity changes caused by a sample in a reactor with different fractions of epithermal neutrons.
3. Activation of sample with and without cadmium covers inside a reactor.

This experiment employs a modification of method 1 which relates the measurement of the reactivity changes to the infinite dilution resonance integral of the sample material. Since the measurements of reactivity were carried out under a cadmium shield which restricts absorption in the sample material primarily to the epithermal neutrons, the introduction of an effective cutoff energy is required. The effective cadmium cutoff energy, E_c , is defined as the energy at which the reactivity change when the actual cadmium cover is present is equal to the reactivity change with an ideal cadmium cover present.

(2) An ideal cadmium cover has an infinite absorption cross section below E_c , and a zero absorption cross section above E_c . In order to use this definition of the effective cadmium cutoff energy it was assumed that E_c was not a function of absorber specie.

A high value of E_c was obtained by Pickard (3), and a part of this research was an attempt to verify those results by using gold plated aluminum powder instead of a copper-gold compound. The experimental procedures used and the preparation of the sample are explained in Chapter 3 and 5 respectively. The ratio of the reactivity worth of gold at infinite dilution to the infinite dilution reactivity worth of boron obtained by Pickard is then used to calculate E_c .

A expression for E_c is derived depending on the form of the adjoint flux or the importance function and using the known measured resonance integral of gold as standard. Once E_c has been determined by this equation, the measured reactivity change of a sample can be related to its unknown resonance integral.

The resonance integral of stainless steel, both 304 and 416, tantalum, and tungsten obtained in this experiment by the expressions derived in Chapter 2 are given in the Results Chapter. These results are compared to the value obtained by the usual method of determining resonance integrals. The discrepancies between the two methods are discussed in the Summary and Conclusion Chapter.

The sources of error in reactivity measurements are discussed in References (4) and (5). The first source of error is a consequence of the statistical fluctuations associated with a finite neutron population. These will ultimately limit the precision of any reactivity measurement. However, in practice a second source of error is encountered due to spurious drifts which will be present in any reactor. These spurious reactivity drifts can be associated with such effects as finite temperature coefficient and are, by definition, not predictable. By assuming that most spurious reactivity drifts occur over fairly a long time intervals and by measuring the period for short duration, the effect of long term spurious drifts could be kept to a minimum. The actual experimental procedures are explained in Chapter 3.

CHAPTER 2

THEORETICAL DEVELOPMENT

The theoretical development is adequately described in reference (3) and will not be presented in detail here. Starting with the energy dependent diffusion equation,

$$\begin{aligned}
 & -\nabla \cdot D(r, E) \nabla \phi(r, E) + \Sigma_T(r, E) \phi(r, E) = \\
 & = \nu Z(E) \int_0^{\infty} \Sigma_f(r, E') \phi(r, E') dE' + \\
 & + \int_0^{\infty} \Sigma_S(r, E') h(E' - E) \phi(r, E') dE'
 \end{aligned} \tag{1}$$

where

$D(r, E)$ = diffusion coefficient at space point r and neutron energy E .

$\phi(r, E)$ = neutron flux at space point r and neutron energy E .

$\Sigma_T(r, E)$ } Total, scattering, and fission macroscopic
 $\Sigma_S(r, E)$ } = cross section at space point r and
 $\Sigma_f(r, E)$ } neutron energy E .

$h(E' \rightarrow E) dE$ = probability that a neutron at E' will be scattered into dE about E .

ν = average number of neutrons produced per fission

$Z(E)$ = energy spectrum of fission neutrons

and with the boundary condition that the neutron flux vanishes at the extrapolated boundary of the reactor, it can be shown from energy-dependent perturbation theory (1) that the reactivity change, $\delta\rho$, due to a small perturbation can be related to $\delta\nu$, with the result that

$$\begin{aligned} \delta\rho &= \frac{\delta\nu}{\nu} \\ &= \frac{\int_0^\infty \int_V \delta\Sigma_a(r,E) \phi(r,E) \phi^+(r,E) \, dr \, dE}{\nu \int_0^\infty \int_{R_V} Z(E) \Sigma_f(r,E') \phi(r,E') \phi^+(r,E) \, dE' \, dr \, dE} \end{aligned} \quad (2)$$

where

$\delta\nu$ = hypothetical change in ν necessary to maintain steady state.

$\phi^+(r,E)$ = the adjoint neutron flux at space point r and neutron energy E .

ν = denotes integration over perturbed volume.

R_V = denotes integrations over entire reactor volume.

The solution of equation 2 is facilitated by considering the ratio of the reactivity effects of two materials, one a resonance absorber and one a $1/\nu$ absorber as (omitting the arguments of variables for convenience),

$$\frac{\delta\rho(\text{res})}{\delta\rho(1/\nu)} = \frac{\int_0^\infty \int_V \delta\Sigma_a(1/\nu + \text{res}) \phi \phi^+ \, dr \, dE}{\int_0^\infty \int_V \delta\Sigma_a(1/\nu) \phi \phi^+ \, dr \, dE} \quad (3)$$

where the absorption cross section has been assumed to consist of two independent parts; a $1/v$ part and a resonance contribution. Since all measurements were performed in the same small test configuration, the spatial effects in $\delta\Sigma_a$, ϕ and ϕ^+ may be considered negligible and the integration over the perturbed volume carried out. Also the measurements were made under a cadmium shield, so the thermal absorption may be considered zero up to some cutoff energy E_c and the ratio of equation

3 written as

$$\frac{\delta\rho(\text{res})}{\delta\rho(1/v)} = \frac{\int_{E_c}^{\infty} N(\text{res}) \sigma_a(1/v + \text{res}) \phi(E') \phi^+(E') dE'}{\int_{E_c}^{\infty} N(1/v) \sigma_a(1/v) \phi(E') \phi^+(E') dE'} \quad (4)$$

Taking the flux in the resonance range to be proportional to $1/E$ and the infinite dilution resonance integral as

$$I = \int_0^{\infty} \frac{\sigma_a(E) dE}{E} \rightarrow \int_{E_c}^{\infty} \frac{\sigma_a(E) dE}{E}$$

equation 4 becomes

$$\frac{\delta\rho(\text{res})}{\delta\rho(1/v)} = \frac{\int_{E_c}^{\infty} N(\text{res}) \sigma_a^{\text{res}}(1/v) \phi^+(E) \frac{dE}{E} + N(\text{res}) \sum_{i=1}^m \phi^+(E_i) I_i}{\int_{E_c}^{\infty} N(1/v) \sigma_a^{1/v} \phi^+(E) \frac{dE}{E}} \quad (5)$$

where $\sigma_a^{\text{res}}(1/v) = 1/v$ portion of neutron capture cross section above E_c .
 $\sum_{i=1}^m \phi^+(E_i) I_i$ = summation of the adjoint flux and resonance integral over the resonance range evaluated at the resonance energy E_i . This is the basic equation used in determining the effective cadmium cutoff energy, E_c , and the resonance integral of various materials.

In order to calculate E_c , gold was used for the resonance absorber because of its known measured resonance integral and boron was used for the $1/v$ absorber. Equation 5 is still impossible to solve unless some form is assumed for the adjoint flux and three forms have been considered.

They are

1. $\phi^+(E) = \text{constant}$
2. $\phi^+(E) \propto 1/E$
3. $\phi^+(E) = \left[\frac{v\Sigma_f(E)}{\Sigma_a(E) + D B^2} \right] \phi_0^+$

where ϕ_0^+ is a normalizing constant and Σ_a , Σ_f , and $D B^2$ are the absorption, fission, and leakage parameters calculated for the unperturbed reactor core. (The derivation of form 3 is in Reference (3).) Substituting the appropriate form for the adjoint flux i.e., ϕ^+ is a constant, and using

$$\sigma_a = \sigma_{aTH} \sqrt{\frac{E_{TH}}{E}}, \text{ and}$$

integrating leads to the following equation,

$$\frac{\delta\rho(\text{Au})}{\delta\rho(\text{B})} = \frac{N_{\text{Au}} \sigma_{\text{TH}}^{\text{Au}}}{N_{\text{B}} \sigma_{\text{TH}}^{\text{B}}} + \frac{N_{\text{Au}} I_T \sqrt{E_c}}{2 N_{\text{B}} \sigma_{aTH}^{\text{B}} \sqrt{E_{TH}}} \quad (6)$$

In the above equation a more accurate value of the total gold resonance integral, I_T , was required than the calculated dilute form (6)

$$I_i = \frac{\pi \sigma_{oi} \Gamma_{\gamma i}}{2 E_i}$$

where

σ_{oi} = peak cross section of resonance

$\Gamma_{\gamma i}$ = total radiative width of resonance

Substituting the constant parameters of Au and B, and the macroscopic cross sections of the TRIGA which are listed in the appendix the following equation is obtained

$$\frac{\rho(\text{Au})}{\rho(\text{B})} = 0.00714 + 0.354 \sqrt{E_c} \quad (7)$$

The above equation determines E_c . Once E_c is determined, an unknown resonance integral can be found from equation 6 with the gold parameters replaced by the unknown. The equation becomes

$$I_u = \frac{2N_B \sigma_{aTH}^B \sqrt{E_{TH}}}{N_u \sqrt{E_c}} \left[\frac{\rho_u}{\rho_B} - \frac{N_u \sigma_{aTH}^u}{N_B \sigma_{aTH}^B} \right] \quad (8)$$

where u refers to the unknown resonance parameters of the sample material.

CHAPTER 3

EXPERIMENTAL PROCEDURE

All reactivity measurements of the samples were performed in the central portion of the TRIGA nuclear reactor. The TRIGA is a 20% enriched uranium fueled, zirconium hydride and water moderated, light water cooled, graphite and water reflected reactor with a maximum operating power level of 100 KW. The reactor is located in the Engineering Building on the campus of The University of Arizona. Part of the experimental apparatus consists of a long aluminum tube, 1 inch in diameter, with a cadmium sleeve. The tube is closed at the bottom and is watertight. The cadmium sleeve is located on the aluminum tube in such a position that when the aluminum tube is extended through the reactor core the cadmium covered region of the tube, approximately four inches long, is in the geometric center of the reactor. The large negative reactivity effect caused by the cadmium sleeve required the TRIGA to have all available fuel elements in the core with the safety and regulating rod fully out and only about 10 cents of the shim rod remaining in the core. This configuration gives a maximum flux symmetry about the central test position.

The other part of the experimental apparatus was the sample holder. This consisted of a solid aluminum rod with two identical sample cavities, that could be inserted into the aluminum tube

described above. These cavities were arranged in such a way that when either sample cavity was in the test position, the other cavity was well outside the active core region. A mechanical positioning device was anchored to the beam directly over the test position to assure that the cavity position could be reproduced.

Once the test apparatus was in place with a sample in one of the cavities, the reactor was brought to critical. The operating power of the reactor was in the region of .15 watts. The low operating power eliminated the temperature and power effects on reactivity. After waiting the required time necessary to eliminate short lived transients, the asymptotic period of the reactor was recorded in the TMC-1024 channel analyzer operating in a multi-scalar mode. The scalar sequentially stored the pulses from the fission chamber in channels of one second duration. Once the series of pulses were recorded, the sample was then lowered from the test position, placing the void cavity in the test position. The sample holder was arranged so that there was no appreciable variation in the amount of aluminum in the reactor during the sample drop or in either position. Again the reactor was allowed to reach its asymptotic period and the data recorded. The procedure was repeated a number of times to achieve statistical accuracy. Each measurement, therefore, consisted of two sets of asymptotic period determinations which could be related to the reactivity of the system through the six group Inhour equation. Subtracting the two reactivity measurements gave the net reactivity worth of the sample.

CHAPTER 4

REACTIVITY MEASUREMENT

At very low reactor power levels the neutron flux in the TRIGA is monitored by the fission chamber. The pulse rate output of this fission chamber was fed into TMC-214 multi-scaler logic unit operating with a TMC-1024 channel analyzer. The pulses from the fission chamber were stored in successive channels, each of one second duration. The resolution time determined for the fission chamber was 20 micro-seconds(3). The TMC-214 multi-scaler unit has a resolution time of 5 micro-seconds and a dead time of 20 micro-seconds per channel associated with the electronic gating. This dead time occurs only at the beginning and end of the one second counting time and therefore, has negligible effect in the overall counting losses of the system. The count rate for this experiment was in the 500-5000 count per second range.

The reactivity was measured for six aluminum-gold samples which varied in the amount of gold present in each sample. The concentration ranged from 55.5 to 628.5 milligrams of gold. From these measurements it was possible to extrapolate the results to determine the infinite dilution reactivity worth of the sample. Once this value was obtained, and using the infinite dilution reactivity worth of boron obtained by Pickard, the cadmium cutoff energy was calculated.

The reactivities were measured for four different types of materials, stainless steel 304 and 416, tantalum, and tungsten to determine the resonance integral of these sample materials.

The asymptotic period of the reactor with the aluminum-gold sample in the test position was measured for 168 seconds. The sample was then taken out of the test position and the void cavity put in. After a waiting time of 3 minutes to eliminate the short lived transients, the asymptotic period was again measured for 168 seconds. This same procedure was used in measuring the tungsten samples. With tantalum in the test position, the asymptotic period was measured for 49 seconds after a 1.5 minute waiting time. The measurement of the asymptotic period of the reactor with stainless steel 304 in the test position was performed on two days. One measurement was for 126 seconds after a waiting time of 2.5 minutes, and the other measurement was for 168 seconds after a waiting time of 3 minutes. For stainless steel 416, the asymptotic period was measured for 168 seconds after a 3 minute waiting time. The waiting time necessary for the reactor to approach an asymptotic period after a prompt reactivity change is discussed in References (5) and (7). The waiting time necessary for the asymptotic period to approach within 1% of its value is on the order of 2.5 minutes for very small reactivity changes. This applies to a source free system and to positive and negative periods if negative periods are longer than 1000 seconds. The shorter waiting time associated with the various samples are justified since waiting times decrease with decreasing period. In the case of tantalum which had

the shortest waiting time of 1.5 minutes only 80 seconds are required to approach the asymptotic period within 1% because its period is on the order of 100 seconds.

After the pulses from the fission chamber were stored in successive channels of the TMC-1024 multi-channel analyzer, the total count for each channel was recorded on a punched paper tape which was then converted to punched cards for analysis using the CDC 6400 digital computer. The actual analysis of the raw data was done using the computer code described in the Computer Code Section. Since the several measurements that were made on one sample gave a range of values, the mean value was assumed to be the reactivity worth of the sample. Although the time span taken to measure the asymptotic period of the sample was short enough to eliminate long term reactivity drifts, short transient drifts were sometimes observed. If the results of the measurement were more than 3 standard deviation removed from the means, it was considered to be the result of a short term spurious drift. The standard deviation is given as(8),

$$\sigma_x = \left(\frac{\sum_{i=1}^n (X_i - \bar{X})^2}{n(n-1)} \right)^{1/2}$$

where

n = number of measurements of X

X_i = observed value of X

\bar{X} = mean of n measurement of X

The reactivity measurements are reported as $\rho \pm \sigma_\rho$

CHAPTER 5

PREPARATION OF SAMPLES

In the preparation of any sample composed of particles of finite size for reactivity measurements, two self-shielding factors must be considered. One is the self-shielding associated with the individual particles that make up the sample, and the other is the self-shielding within the sample consisting of these particles. The self-shielding within the particles is discussed in the self-shielding appendix. These were found to be negligible. The self-shielding within the sample was determined by measurements and using varying concentrations of the particles then extrapolating the results to the zero concentration to allow the change in reactivity per unit mass to be derived at the infinite dilution point.

The material chosen as the known resonance absorber for this experiment was gold. Since self-shielding within any obtainable macroscopic pure gold particle is significant, either the gold particles must be in a gold compound or in a microscopic state.

First the desired amount of gold, 1.53515 grams, was weighed to an accuracy of 0.00005 grams and the gold then dissolved in 5 ml. of aqua regia. The resulting solution was mixed with water and poured into a mixture of fine aluminum powder and water. This was stirred continually for about 2 hours. Because the aluminum is a reducing agent, the

gold will plate onto the aluminum particles. Aluminum powder was chosen for the diluent material for the gold samples because of its very low capture cross section. After the mixture was thoroughly mixed, it was baked for approximately 10 hours at about 110°C. This mixture was then ground to a fine powder with a mortar and pestle and weighed. The desired amount of gold to be put into the sample was determined by weighing an amount of gold plated aluminum powder and using the formula

$$\left(\begin{array}{l} \text{weight of gold to} \\ \text{be put in sample} \end{array} \right) = \frac{\left(\begin{array}{l} \text{weight of gold in mixture} \\ \text{weight of mixture} \end{array} \right)}{\left(\begin{array}{l} \text{weight of mixture} \\ \text{to be put in sample} \end{array} \right)} \quad (9)$$

The weight of the gold plated aluminum powder to be put into the sample was less than the required 9 grams to make the sample. (The amount of pure aluminum diluent necessary to make the sample was determined by making a dummy sample.) Pure aluminum powder was added to the gold plated aluminum powder until the final weight was about 9 grams. This mixture of gold plated aluminum powder and pure aluminum powder was mixed together in a mixing tube and shaken vigorously for approximately 30 minutes. After the powder was thoroughly mixed, it was poured into a mold and pressed into a solid right cylindrical pellet, 5/8" in diameter and approximately 1" in height. Pictures and a detailed description of the mold and press assembly are given in Reference 3. The sample was then removed from the mold and sintered at approximately 500°C for 2 days. Since there was a small amount of spill in putting the aluminum and gold plated aluminum mixture in the mold assembly, the final amount of gold in the sample was determined from the same type of formula as (9).

The shape of three of the other sample materials which were used to determine the unknown resonance integrals were also solid right cylinders. The fourth was a hollow right cylinder. The dimensions are tabulated below.

TABLE I
SAMPLE DIMENSIONS AND WEIGHTS

Sample	Diameter (in.)	Height (in.)	Weight (gr.)
Stainless steel 304	0.625	1.130	44.652
Stainless steel 416	0.500	1.000	24.462
Tantalum	0.630	1.505	126.528
Tungsten	0.500 (OD) 0.265 (ID)	1.475	65.179

CHAPTER 6

RESULTS

The results of the reactivity measurements for the six gold samples are given below in Table II. The corrections to the measurements for the self-shielding within the individual particles that made up the sample were negligible. (See Self-Shielding Appendix.)

TABLE II
REACTIVITY MEASUREMENTS OF GOLD SAMPLES

Sample No.	Gold Wt. (mg)	Aluminum Wt. (gm)	Reactivity Worth (cents)
1	55.5	8.747	.112 \pm .071
2	78.0	8.537	.143 \pm .064
3	105.9	9.629	.223 \pm .038
4	212.0	7.742	.255 \pm .087
5	418.9	6.520	.272 \pm .061
6	628.5	5.381	.440 \pm .071

The reactivity measurements of the gold samples were corrected for the aluminum diluent. The corrections were made by multiplying the reactivity worth per gram of aluminum by the amount of aluminum in the actual sample. (The aluminum had a reactivity effect of 0.0042 ϵ /gm(3).) Since aluminum had an opposite effect on the reactivity relative to the gold, the aluminum reactivity corrections were added to the gold reactivity. The aluminum corrections and corrected reactivities are listed in Table III.

TABLE III
REACTIVITY CORRECTIONS

Sample No.	Aluminum Correction (cents)	Corrected Reactivity (cents)
1	.037	.149 \pm .074
2	.036	.179 \pm .066
3	.41	.263 \pm .042
4	.032	.287 \pm .092
5	.027	.300 \pm .065
6	.023	.463 \pm .075

These corrected values of the reactivity worth of gold vs the mass of gold are plotted in Figure 1. The theoretical curve fitted to the data is based on Wigner's Rational Approximation for escape probability, which is discussed in Reference (3). The form of the theoretical curve is

$$\rho = \rho_0 \left(\frac{M}{A+M} \right)$$

where

ρ = corrected reactivity worth of sample

M = mass of absorber in sample

A
} = constant parameters of the curve
 ρ_0

The infinite dilution worth of an absorbing material is then found from,

$$\left(\frac{d\rho}{dM} \right)_{M=0} = \frac{\rho_0}{A}$$

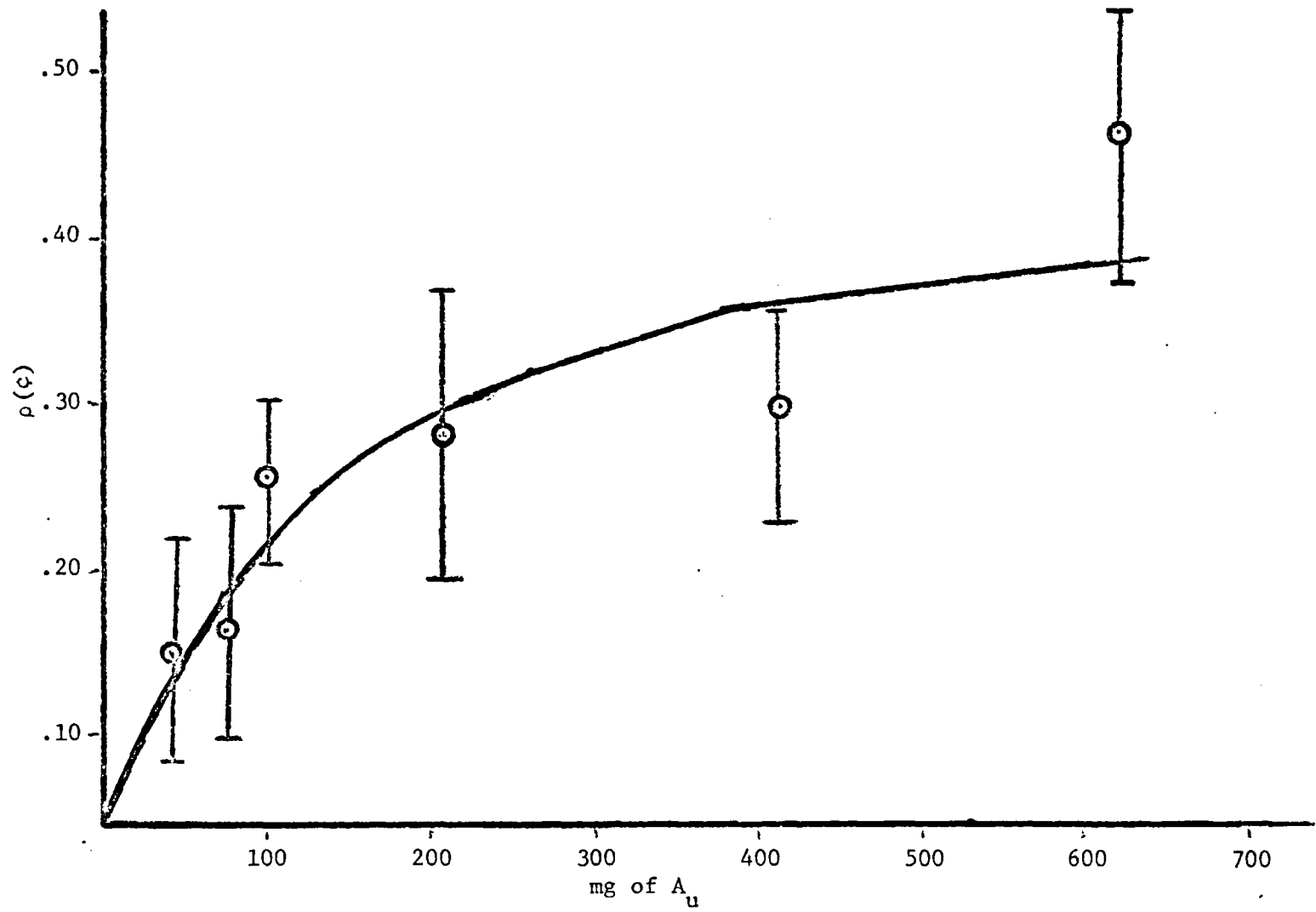


FIGURE 1: Measured Reactivity versus Mass of Gold

The gold curve is described by

$$\rho_{\text{Au}} = 0.482 \left(\frac{M}{124.0 + M} \right)$$

and the infinite dilution reactivity worth of gold is,

$$\left(\frac{d\rho}{dM} \right)_{M=0} = 3.89 \text{ } \zeta/\text{gram}$$

The infinite dilution reactivity of boron obtained by Pickard is 13.14 ζ/gram . The ratio of the infinite dilution worth of gold and boron is

$$\frac{\rho_{\text{Au}}}{\rho_{\text{B}}} = 0.296$$

as compared to 0.417 obtained by Pickard.

The value of E_c as calculated using the above data is then

$$E_c = 0.665 \text{ ev.}$$

In the TRIGA, the energy dependence of the adjoint flux over the resonance region is best described as a constant, so the cadmium cutoff energy is 0.665 ev. Using this value for the cutoff energy, the unknown resonance integrals are then found from

$$I_u = \frac{2N_B \sigma_{aTH}^B \sqrt{E_{TH}}}{N_u \sqrt{E_c}} \left[\frac{\rho_u}{\rho_B} - \frac{N_u \sigma_{aTH}^u}{N_B \sigma_{aTH}^B} \right] = \frac{16.50}{N_u} \left[\frac{\rho_u}{13.14} - \frac{N_u \sigma_{aTH}^u}{42.28} \right] \quad (10)$$

Equation (10) was used to calculate the infinite dilution resonance integral of four sample materials. The results of this calculation, and the measured reactivity per gram are shown in Table IV.

TABLE IV

REACTIVITY MEASUREMENTS OF SAMPLE MATERIALS

Sample Material	Reactivity per gm. (cents) 10^{-3}	I (barns) Eq. 5
Tantalum	80.23 ± 1.16	22
Tungsten	45.49 ± 5.12	10
Stainless Steel 304	7.17 ± 0.94	-0.35
Stainless Steel 416	5.65 ± 4.68	-0.60

CHAPTER 7

SUMMARY AND CONCLUSION

When the calculated values of the infinite dilution resonance integrals are compared to the accepted values of the infinite dilution resonance integrals that are listed in Reference (9) it is apparent that the method used in this thesis of determining resonance integrals applies only for materials that have large resonance integrals compared to the $1/v$ contribution. In the cases where the sample materials have large resonance integrals, either a self-shielding factor must be calculated to determine the flux depression within the sample or self-shielding curves must be made that are the same type as Figure I of Chapter 6. The calculation of a self-shielding factor for a sample with an unknown resonance is somewhat of a problem. Even if the resonance parameters were known, it would be difficult to determine an average absorption cross section over the resonance region.

In Table IV some justification needs to be made for the negative values of the resonance integral of the stainless steels calculated from Equation 10. In the case of stainless steel 416, the large standard deviation of the reactivity measurement could account for the negative result. This isn't the case for stainless steel 304. The standard deviation is small enough that when the highest possible value of the reactivity is considered the result is still negative.

(The reactivity worth per gram of stainless steel 304 obtained by this author was compared to the value in Reference 10, the two values were in agreement.)

The negative result comes from subtracting the $1/v$ contribution to the resonance integral. Above the cadmium cutoff energy this term should be negligible. For materials that have small reactivity effect, this term is not only significant, but as in the case of the stainless steel the term is dominant.

APPENDIX I

SELF-SHIELDING

In preparing the experimental samples of gold, it was desirable to have a particle small enough so self-shielding within the particle could be neglected. A self-shielding factor may be defined as

$$f_o = \frac{\text{average flux throughout absorber}}{\text{average flux at surface of absorber}}$$

This is identical to the average escape probability, P_o .

In the case of a slab, using transport theory and Dirac Chord method, the result is

$$P_o = \frac{\ell}{a} \left(\frac{1}{2} - E_3\left(\frac{a}{\ell}\right) \right)$$

where

$$l = \frac{1}{\Sigma_a}$$

a = thickness of slab

For a 90% escape probability at the peak of the resonance cross section, the thickness of the slab must be less than 3.19×10^{-5} cm. Since the escape probability is a function of the geometry of the particles and does not depend on neutron energy, P_o was redefined to obtain an average over the resonance energy range as

$$P_o = \frac{\int_{\text{Res}} P(E) dE}{\int_{\text{Res}} dE} \quad (11)$$

The range of integration was determined by defining a practical width of resonance, Γ_p . The practical width of a resonance is defined as the energy interval over which the resonance cross section, i.e., the sum of the cross section for resonance absorption and resonance scattering, is greater than the macroscopic potential scattering cross section. (1) This can be expressed as

$$\Gamma_p = \Gamma \sqrt{\frac{N_A \sigma_1}{\Sigma_p}}$$

where

Γ = level width

Σ_p = macroscopic potential scattering cross section
of the mixture

$$= N_A \sigma_{PA} + N_M \sigma_{SM}$$

N_A and N_M are the atom density of the absorber and moderator, respectively, σ_{PA} is the potential scattering cross section of the absorber, and σ_{SM} is the scattering cross section of the moderator. By substituting the appropriate expressions for $P(E)$ and $\sigma_a(E)$ into equation 11 and integrating over the resonance range, a correction factor was found that was much smaller than the experimental accuracy.

APPENDIX II

COMPUTER PROGRAM

Two computer codes, REACTIVITY and SELF-SHIELD, were used in the analysis of the data obtained in this experiment. REACTIVITY took the raw data and converted it to the net reactivity worth of the sample in the following manner. After the counts from the 1024 multi-channel analyzer were converted to EDPM input and compiled by the computer, the count rate was corrected for the 20 micro-second dead time associated with the fission counter by the formula,

$$n_o = \frac{n}{1-n\tau}$$

n_o = true count rate

n = observed count rate

τ = dead time

By assuming that the neutron population varied asymptotically with time,

$$P = N e^{-t/T}$$

P = neutron population at time t

N = neutron population at time $t = 0$

T = asymptotic period

$$= 1/W$$

REACTIVITY Made a least square fit to the n separate corrected count rates with an exponential curve as a first approximation. The inverse slope or the asymptotic period and N is given respectively by,

$$W_o = \frac{1}{T_o}$$

$$= \frac{\sum_{i=1}^n (it) \sum_{i=1}^n \ln N_i - n \sum_{i=1}^n (it) \ln N_i}{\left(\sum_{i=1}^n (it) \right)^2 - n \sum_{i=1}^n (it)^2}$$

where

t = actual time that the pulses were counted

= 1 second

N_i = corrected observed count rate at time i t

$$\ln N_o = \frac{\sum_{i=1}^n (it) \sum_{i=1}^n it \ln N_i - \sum_{i=1}^n \ln N_i \sum_{i=1}^n (it)^2}{\left(\sum_{i=1}^n (it) \right)^2 - n \sum_{i=1}^n (it)^2}$$

Because the method of least squares does not give the "best fit" to an exponential curve, these values of W_o and N_o were taken as initial estimates of W and N (11). By a process of iteration the best fit to exponential curve can be obtained from the following formulae.

$$W = \frac{\sum_{i=1}^n N_o ite^{2\omega_o it} \sum_{i=1}^n e^{\omega_o it} (N_o e^{\omega_o it} - N_i) - \sum_{i=1}^n e^{2\omega_o it} \sum_{i=1}^n N_o ite^{\omega_o it} (N_o e^{\omega_o it} - N_i)}{\sum_{i=1}^n e^{2\omega_o it} \sum_{i=1}^n N_o^2 (it)^2 e^{2\omega_o it} - \sum_{i=1}^n N_o ite^{2\omega_o it} \sum_{i=1}^n N_o ite^{2\omega_o it}} + W_o$$

and

$$N = \frac{\sum_{i=1}^n N_o ite^{2\omega_o it} \sum_{i=1}^n N_o ite^{\omega_o it} (N_o e^{\omega_o it} - N_i) - \sum_{i=1}^n N_o^2 (it)^2 \sum_{i=1}^n e^{\omega_o it} (N_o e^{\omega_o it} - N_i)}{\sum_{i=1}^n e^{2\omega_o it} \sum_{i=1}^n N_o^2 (it)^2 e^{2\omega_o it} - \sum_{i=1}^n N_o ite^{2\omega_o it} \sum_{i=1}^n N_o ite^{2\omega_o it}} + N_o$$

Once W_o and N_o are not appreciably different from W and N, the reactivity was calculated from the six group inhour equation.

$$\rho = \frac{\lambda\omega + \sum_{i=1}^6 \frac{\beta_i \omega}{\omega + \lambda_i}}{1 + \lambda\omega}$$

where

l = prompt neutron lifetime

= 80 micro-second for TRIGA

β_i = delayed fraction of i^{th} group

λ_i = decay rate of i^{th} group precursor

ω = $1/T$

ρ = reactivity

The β_i and λ_i used were from Keepin six group parameters for U^{235} (12). By subtracting the reactivity measured with the sample in the test position from the reactivity measured with the void in the test position, the net reactivity worth of the sample was determined. Since the net reactivity worth of the sample was measured a number of times, the sample worth could be reported as plus or minus a standard deviation.

For the gold samples, the reactivity was corrected to account for the aluminum in the sample. Then the computer code, SELF-SHIELD, using the corrected reactivity made a best fit of these data to the self-shielding curve

$$\rho = \rho_0 \frac{M}{A + M}$$

where

ρ = corrected reactivity worth of samples

M = absorber mass of sample

ρ_0, A = curve parameters

This equation is derived in Reference 3. The best fit to the self-shielding curve was obtained by noting that errors between the measured quantities ρ_i and M_i and the theoretical curve are given by

$$\epsilon_i = \rho_i - \frac{\rho_o M_i}{A + M_i}.$$

Let

$$S = \sum_{i=1}^n \epsilon_i^2$$

then the normal equations for determining the best fit values for A and ρ_o are

$$\left(\frac{\partial S}{\partial A}\right) = 0$$

$$\left(\frac{\partial S}{\partial \rho_o}\right) = 0$$

Since these equations cannot be solved explicitly for A and ρ_o , a first order minimization σ_i was employed.

$$\begin{aligned} \sigma_i &= \epsilon_i (A + M_i) \\ &= \rho_i (A + M_i) - \rho_o M_i. \end{aligned}$$

The solution to the normal equation obtained for this error was incremented until the true minimum for the least square error was found.

The first order normal equations are:

$$A = \frac{\sum_{i=1}^n (M_i \rho_i^2) \sum_{i=1}^n (M_i)^2 - \sum_{i=1}^n (M_i^2 \rho_i) \sum_{i=1}^n (M_i \rho_i)}{(\sum_{i=1}^n M_i \rho_i)^2 - \sum_{i=1}^n (\rho_i)^2 \sum_{i=1}^n (M_i)^2}$$

and

$$\rho_o = \frac{\sum_{i=1}^n (M_i^2 \rho_i) \sum_{i=1}^n (\rho_i)^2 - \sum_{i=1}^n (M_i \rho_i^2) \sum_{i=1}^n (M_i \rho_i)}{\sum_{i=1}^n (M_i)^2 \sum_{i=1}^n (\rho_i)^2 - (\sum_{i=1}^n (M_i \rho_i))^2}$$

These differed by only a few percent from the parameters of the true least squares curve. The infinite reactivity value of an absorbing material is found from

$$\left(\frac{\partial \rho}{\partial M}\right)_{M=0} = \frac{\rho_o}{A}$$

APPENDIX III

ADJOINT FLUX

The evaluation of resonance cross section parameters from reactivity measurements requires a knowledge of the TRIGA adjoint fluxes. Analytic approximations are available only in limited cases making it necessary to utilize multigroup diffusion calculations. In the case of TRIGA, multigroup adjoints have been evaluated with a 23 energy group diffusion code called DUST. Fast neutron cross sections were calculated from 1 ev to 10 Mev with GAM, a P_1 or B_1 transport code. A thermal group was calculated with TEMPEST, using the Wigner-Wilkins equations. The energy dependence of the adjoint flux for TRIGA was found to be nearly constant in the resonance range of energies which allowed the adjoint flux to be treated as independent of energy. The TRIGA adjoint fluxes in the "C" ring and sample position are shown in Figure

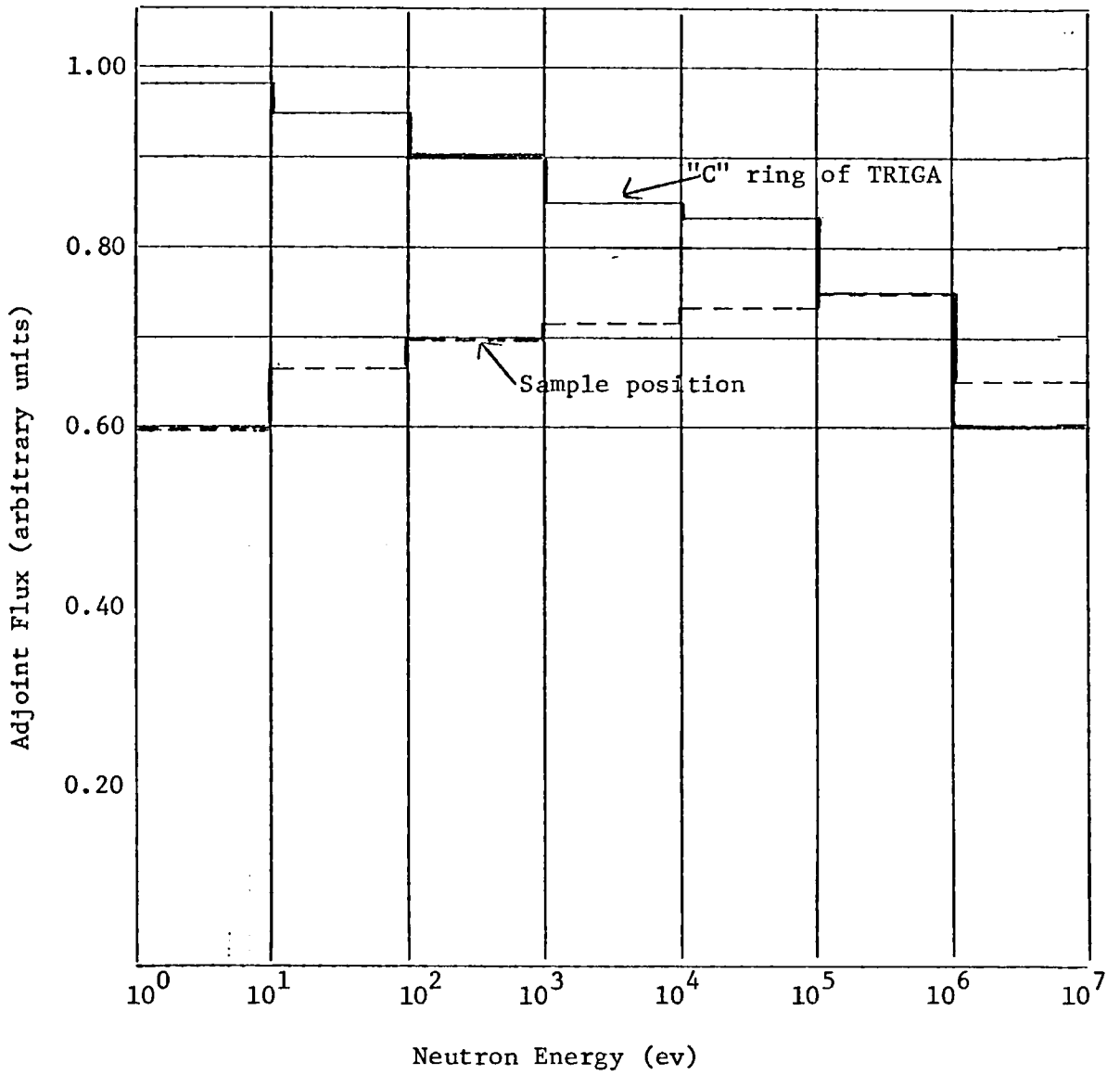


FIGURE 2: Adjoint Flux versus Neutron Energy

APPENDIX IV

PARAMETERS OF MATERIALS USED IN CALCULATIONS

Boron $N_B = 5.571 \times 10^{22}$ atom/gram

$$\sigma_{aTH}^B = 759 \pm 2.0 \text{ barns}$$

Gold $N_{AU} = 3.058 \times 10^{21}$ atom/gram

$$\sigma_{aTH}^{Au} = 98.8 \pm 0.3 \text{ barns}$$

$$I_T = 1558 \text{ barns}$$

$$\sum_{i=1}^n I_i = 1056.9 \text{ barns}$$

Tantalum $N_{Ta} = 3.328 \times 10^{21}$ atom/gram

$$\sigma_{aTH}^{Ta} = 21 \pm 3.0 \text{ barns}$$

Tungsten $N_u = 3.276 \times 10^{21}$ atom/gram

$$\sigma_{aTH}^W = 19 \pm 0.5 \text{ barns}$$

Stainless Steel 304 $N = 1.100 \times 10^{22}$ atom/gram

$$\sigma_{aTH} = 3.01 \pm 0.36 \text{ barns}$$

Stainless steel 416

$$N = 1.110 \times 10^{22} \text{ atom/gram}$$

$$\sigma_{aTH} = 3.18 \pm 0.37 \text{ barns}$$

Miscellaneous

$$\phi_{AT} = 0.5671 \text{ cm}^{-1}$$

$$\phi_{BT} = 0.2030 \text{ ev}^{-1}$$

TRIGA

$$\Sigma_{aTH} = 0.0815 \text{ cm}^{-1}$$

$$\Sigma_{fTH} = 0.0553 \text{ cm}^{-1}$$

$$D = 0.301 \text{ cm}$$

$$B^2 = 38 \times 10^{-4} \text{ cm}^{-2}$$

$$K = .0882 \text{ ev}^{-1}$$

TABLE V

PARAMETERS OF RESOLVED GOLD RESONANCE

E_0 (eV)	Γ_γ (eV)	σ_0 (b)	I_i (b)
4.906	.124	26500	1052.107
58.1	.112	145	.439
60.25	.130	1000	3.389
78.4	.140	150	.421
107.0	.120	98	.173
144.2	.120	31	.041
151.3	.120	80	.100
164.9	.106	110	.111
190.3	.130	64	.069
240.5	.100	72	.047

REFERENCES

1. Lamarsh, John R. Introduction to Nuclear Reactor Theory. Reading, Massachusetts: Addison-Wesley Publishing Company, Inc., 1966.
2. Brown, H. L. and T. J. Connelly. "Cadmium Cutoff Energies for Resonance Absorbers in Activation and Reactivity Measurements," Nuclear Science and Engineering, Vol. 24, p. 6 (1966).
3. Pickard, Paul S. Reactivity Measurements of Cross Sections in Epicadmium Regions. Thesis, University of Arizona, 1966.
4. Bennett, Edgar F. and Robert L. Long. "Precision Limitations in the Measurement of Small Reactivity Changes," Nuclear Science and Engineering, Vol. 17, p. 425 (1963).
5. Toppel, B. J. "Sources of Error in Reactivity Determination by Means of Asymptotic Period Measurements," Nuclear Science and Engineering, Vol. 5 (1959).
6. Dresner, L. Resonance Absorption in Nuclear Reactors. New York: Pergamon Press, 1960.
7. Argonne National Laboratory. Reactor Physics Constants, ANL-5800 United States Atomic Energy Commission, 1963.
8. Young, Hugh D. Statistical Treatment of Experimental Data. New York: McGraw-Hill Book Company, Inc., 1962.
9. Etherington, Harold. Nuclear Engineering Handbook. New York: McGraw-Hill Book Company, Inc., 1958.
10. Fast, E., C. L. Beck, D. A. Millsap, R. G. Nisle, J. W. Rogers, and J. J. Scoville. "Use of the ARMOR for a Fast Reactor Support Program," Idaho Nuclear Corporation. Idaho Falls, Idaho.
11. Wylie, C. R., Jr. Advanced Engineering Mathematics. New York: McGraw-Hill Book Company, Inc., 1960.
12. Keepin, G. R., T. F. Wimett, and R. K. Zeigler. "Delayed Neutrons from Fissionable Isotopes of Uranium, Plutonium, and Thorium," Phys. Rev., Vol. 107, p. 1044 (1957).